HHS Public Access

Author manuscript

Eur Radiol. Author manuscript; available in PMC 2019 March 01.

Published in final edited form as:

Eur Radiol. 2018 March ; 28(3): 936–945. doi:10.1007/s00330-017-5062-y.

Differentiation of Benign and Malignant Solid Pancreatic Masses Using Magnetic Resonance Elastography with Spin-echo Echo Planar Imaging and Three-dimensional Inversion Reconstruction: A Prospective Study

Yu Shi, M.D.[1], **Feng Gao, M.S.**[2], **Yue Li, M.S.**[3], **Shengzhen Tao, M.S.**[4], **Bing Yu, M.D.**[1], **Zaiyi Liu, M.D.**[5], **Yanqing Liu, M.S.**[1], **Kevin J. Glaser, Ph.D.**[4], **Richard L. Ehman, M.D.**[4], and **Qiyong Guo, M.D.**[1,*]

[1]Department of Radiology, Shengjing Hospital of China Medical University, Shenyang, P.R. China

[2]Department of Hepato-pancreato-biliary Tumour Surgery, Shengjing Hospital of China Medical University, Shenyang, P.R. China

[3]Department of Pathology, Shengjing Hospital of China Medical University, Shenyang, P.R. China

[4]Department of Radiology, Mayo Clinic, Rochester, MN

[5]Department of Radiology, Guangdong General Hospital, Guangdong Academy of Medical Sciences, Guangzhou, P.R. China

Abstract

Objectives—To determine the diagnostic performance of MR elastography (MRE) and compare it with serum CA19-9 in differentiating malignant from benign pancreatic masses, with emphasis

Corresponding author: Qiyong Guo M.D., Professor of Radiology, Department of Radiology, Shengjing Hospital of China Medical University, No.36, Sanhao Street, Heping District, Shenyang, 110004, P.R. China, guoqiyongcmu@163.com, Phone:86-24-83956966, Fax: 86-24-23929902.

Compliance with ethical standards:

Guarantor:

The scientific guarantor of this publication is Qiyong Guo.

Conflict of interest:

The authors of this manuscript declare relationships with the following companies: Kevin J. Glaser has stock in Resoundant and intellectual property related to MR elastography. He has a patent and receives licensing royalties through Resoundant and GE Medical Systems. Richard L. Ehman is an equity holder in and chief executive officer of Resoundant. He has a patent and receives licensing royalties for MR elastography.

Statistics and biometry:

Bing Ma kindly provided statistical advice for this manuscript.

Ethical approval:

Institutional Review Board approval was obtained.

This research was approved by the Institutional Review Board of Shengjing Hospital of China Medical University and conducted in accordance with the Declaration of Helsinki and its amendments, and Good Clinical Practice guidelines.

Informed consent:

Written informed consent was obtained from all subjects (patients) in this study.

Methodology:

- prospective
- diagnostic or prognostic study
- performed at one institution

on differentiating between pancreatic ductal adenocarcinoma (PDAC) and mass-forming pancreatitis (MFP).

Methods—We performed a prospective, consecutive, 24-month study in 85 patients with solid pancreatic masses confirmed by histopathologic examinations. The mass stiffness and stiffness ratio (calculated as the ratio of mass stiffness to the parenchymal stiffness) were assessed. The diagnostic accuracy was analysed by calculating the area under the ROC curve (AUROC).

Results—The final diagnosis included 54 malignant tumours (43 patients with PDAC) and 31 benign masses (24 patients with MFP). The stiffness ratio showed better diagnostic performance than the mass stiffness and serum CA19-9 for the differentiation between malignant and benign masses (AUC: 0.912 vs 0.845 vs 0.702; P= 0.026, P< 0.001) and, specifically, between PDAC and MFP (AUC: 0.955 vs 0.882 vs 0.745; P= 0.026, P=0.003). The sensitivity, specificity and accuracy of stiffness ratio for the differentiation of PDAC and MFP were all higher than 0.9.

Conclusions—MRE presents an effective and quantitative strategy for non-invasive differentiation between PDAC and MFP based on their mechanical properties.

Keywords

Diagnostic performance; Elastography; Magnetic resonance imaging; Pancreatic Neoplasms; Pancreatitis, Chronic

Introduction

Solid pancreatic masses, which cover a wide spectrum of pancreatic anomalies, can be classified as benign lesions (e.g., mass-forming pancreatitis [MFP], lipoma, hamartoma, fibroma and solid pseudopapillary neoplasm [SPN]) or malignant neoplasms (e.g., pancreatic cancer, metastatic tumour, primary pancreatic lymphoma and neuroendocrine pancreatic tumour [NEPT]) [1–4]. Pancreatic ductal adenocarcinoma (PDAC), which accounts for 85–90% of all malignant pancreatic tumours, is one of the five most lethal malignancies worldwide [5]. Currently, its early detection is essential for complete R0 surgical resection (defined as resection for cure or complete remission), which is believed to be the best curative option for improving prognosis [6]. Differentiation between PDAC and MFP remains challenging because of significant overlap in radiological findings (e.g., focal solid mass around the head of the pancreas, double duct obstruction, and absence of hypervascularity) [7–10], and unless imaging shows definite features of malignancy, such as signs of vascular invasion or liver metastases, the diagnostic performance of conventional imaging remains inadequate for definitive differentiation between PDAC and MFP. Other solid pancreatic masses such as non-functioning NEPT and small SPNs are also prone to misdiagnosis as PDAC or other pancreatic malignancy [11]. Computed tomography (CT)- or endoscopic ultrasound (EUS)-guided biopsy can provide cytological samples for definitive diagnosis of pancreatic lesions. However, these procedures are invasive, the samples may not be sufficient, and the small, but not negligible, risk of morbidity cannot be ignored [12]. Serum carbohydrate antigen 19-9 (CA19-9) may be useful for monitoring PDAC, but it is neither specific nor sensitive for initial diagnosis of PDAC, yielding both false-negative results among patients without 1, 4-fucosyltransferase enzyme activity and false-positive

results patients with non-malignant conditions including cholelithiasis, liver cirrhosis, and chronic pancreatitis [13; 14].

Magnetic resonance elastography (MRE) is an MR-based technique that was developed for quantitative assessment of tissue stiffness based on mapping the propagation of shear waves in tissue [16]. MRE has been widely utilised to accurately stage hepatic fibrosis and to differentiate benign from malignant focal liver diseases [17–21]. Histologically, PDAC is a hard mass characterised by a marked desmoplastic reaction and build-up of fibrotic tissues [22]. MFP is also characterised by perilobular fibrosis, but with significantly lower mean collagen content compared with pancreatic carcinoma or tumour-associated chronic pancreatitis [23; 24], which suggests that the stiffness of MFP should be less than that of PDAC [17; 22; 25; 26]. Previous elastography studies based on EUS have indicated that the stiffness ratio between tumour and surrounding parenchyma is a useful metric for differentiating solid pancreatic masses [27; 28]. Hence, we hypothesised that MRE assessment of both mass stiffness and the stiffness ratio would present an opportunity for differentiation of malignant from benign pancreatic masses, particularly PDAC from MFP, based on tissue mechanical information.

MR imaging using 40-Hz vibrations and a spin-echo echo-planar imaging (SE-EPI) pulse sequence with three dimensional (3D) motion encoding was recently shown to provide robust estimates of tissue shear stiffness in healthy pancreas, presenting a better wave pattern and higher amplitude of motion when compared with imaging at 60-Hz [29]. 3D SE-EPI MRE acquisition and stiffness calculation algorithm is designed for applications to small and/or geometrically complex organs including pancreas, brain, and breast [16; 29]. To our knowledge, no study has been conducted to evaluate the usefulness of 3D SE-EPI MRE for differentiation of solid pancreatic masses. Thus, the purpose of our study was to determine the diagnostic performance of 3D SE-EPI MRE and compare it with serum markers (CA19-9) in differentiating malignant from benign masses, with emphasis on the differential diagnosis between PDAC and MFP.

Materials and Methods

Subjects

A prospective, consecutive, 24-month study was designed to assess the clinical performance of MRE-measured pancreatic stiffness in the differential diagnosis of solid pancreatic masses. The study was approved by the local institutional review board and conducted in accordance with the Declaration of Helsinki and its amendments, and Good Clinical Practice guidelines. The nature of MRE was explained in detail and written informed consent was obtained from all subjects.

Patient group: Consecutive patients suspected of having solid pancreatic masses based on CT/MR/ultrasound results in the local department of Radiology and Ultrasound from December 2013 to December 2015 were recruited. Two hundred and fifty-four patients were enrolled, and 169 were excluded ultimately based on the criteria described in the flow diagram (Figure 1) and in the Supplementary Appendix. Malignancy was confirmed by histological examination of surgical specimens or a definitely positive cytology for

malignancy together with compatible imaging findings. Benign diseases were diagnosed by histological examination of surgical specimens or imaging (EUS or CT/MR) findings at entry, clinical presentation and a minimum 6-month follow-up period that included at least one EUS-guided fine-needle aspiration (FNA) biopsy showing benign cytology. Among the 123 patients without confirmed histopathological diagnosis, 86 subjects had neither post-resection pathology nor cytological results, and 37 were initially diagnosed with benign masses, but failed to have adequate follow-up time for definitive exclusion of malignancy. In the end, 85 patients (mean age, 54.0±12.1years; range, 21–80 years; 58 men and 27 women; mean BMI, 21.1±2.7kg/m^2) who had histological results and proper MRE stiffness estimates available, were included. The patients' demographics and baseline characteristics were all recorded before surgery or at the time of biopsy, as shown in Table 1.

Control group: twenty healthy volunteers (mean age, 52±10.6 years; range, 31–69 years; 13 men and 7 women; mean BMI, 23.2±4.3kg/m^2) were recruited from the nearby community as controls during the study period, compiling the stiffness of the healthy pancreas. None of the healthy volunteers had history of pancreatic disease, symptoms of maldigestion, history of alcohol or tobacco abuse [30], or increased serum levels of pancreatic enzymes.

Image acquisition

All examinations were performed on an MR Scanner (Signa HDX 3.0T system; GE Healthcare, Milwaukee, WI) equipped with an eight-channel phased-array body coil. All subjects were instructed to fast for 2 to 3 hours before the examination. An ergonomic soft pancreatic MRE passive driver [29] was placed against the upper abdomen, centred on the xiphisternum, and secured with a 20-cm–wide elastic band that wrapped around the body to ensure good coupling between the driver and the body. External mechanical shear waves, 40-Hz, were generated using an active acoustic actuator located outside the MR scanner room and were introduced into the upper abdomen via a 5-m flexible vinyl tube terminating in the passive driver, as described in literature [29]. All subjects were imaged in a supine position, feet first, with a 32-slice, flow-compensated, SE-EPI pulse sequence modified to include additional MRE motion-encoding gradients (MEGs) alternating in positive and negative x, y, and z directions to record full-vector tissue motion into the phase of the MR images. The acquisitions were performed at the end of expiration during 5 periods of suspended respiration (4 × 22 s and 1 × 11 s). The imaging parameters for 3D SE-EPI MRE were as follows: repetition time/echo time = 1375/38.8 ms; phase offsets = 3; field of view = 32 to 38 cm; acquisition matrix = 96 × 96; parallel imaging acceleration factor = 3; slice thickness = 3 to 3.5 mm; in-plane resolution = 3.3 × 3.3 mm to 3.9 × 3.9 mm. We also performed axial T1-and T2-weighted scans with/without fat suppression and coronal scans. The imaging parameters are given in Supplementary Table 1.

A comfort scale rating of the MRE exam was subsequently obtained based on patient experience. Each patient completed a questionnaire, scoring the test for comfort and acceptance level on a scale of 1 (intolerable) to 5 (very satisfactory).

Image analysis

The post-processing software was supplied by the Mayo Clinic, Rochester MN, along with the MRE pulse sequence. The acquired wave images were processed automatically on the scanner to generate quantitative images depicting tissue stiffness maps (elastograms) using the inversion algorithm previously described for healthy pancreas [29]. A 3D direct inversion of the Helmholtz wave equation using the curl of the measured wave fields and 3D directional filtering were performed to generate elastograms from the wave images. MR magnitude images were also obtained from the MRE images, showing anatomical information coregistered with the wave images and elastograms to be used for localisation of anatomical features. Regions of interest (ROIs) were drawn on the magnitude images to encompass as much of the mass as possible while avoiding the borders to reduce boundary effects. The ROIs were transferred to the elastograms to obtain the tissue stiffness (i.e., tissue elasticity modulus) in the units of kilopascals. Image slices containing the mass were selected in a slice-by-slice fashion with one ROI for each slice and mean stiffness of each mass was calculated as the average of the stiffness values from the pooled slices containing the mass. The stiffness of extralesional pancreatic parenchyma was calculated by averaging the stiffness from 2 to 3 ROIs (one ROI for each slice, >300 mm^2) in the parenchyma across its largest dimension in 2 to 3 consecutive slices, away from mass, borders, and large vessels. ROIs in both masses and parenchyma were oval or geographic in shape. The stiffness ratio was calculated as the stiffness of the pancreatic mass/the stiffness of the pancreatic parenchyma.

The MRE images were interpreted by a primary reader (4 years of experience interpreting MRE) and a secondary reader (2 years of MRE experience) who were not aware of the final diagnosis of the solid masses. Stiffness measurements were performed twice, with an interval of at least 4 weeks between evaluations to avoid memory bias. Intra- and inter-reader agreements were calculated, and after testing the reproducibility of the stiffness measurement, the results from the primary reader were utilised for all subsequent analysis.

Histopathologic assessment

The median interval between surgery/biopsy and MR examinations was 4 days (range 1 to 21 days), and in 80 patients (94.1%) the interval was ≤7 days. FNA or surgical specimens were examined by staining with haematoxylin/eosin (H&E) and by immunohistochemistry for cytokeratin, CD56, chromogranin, and synaptophysin for neuroendocrine tumours, thyroid transcription factor-1 for lung cancer, cytokeratin 20, villin, and CDX-2 for colon cancer, and β-catenin, AACT, vimentin, synaptophysin, cytokeratin, and ki67 for SPN. The histopathologic analysis was performed in consensus by two experienced pathologists with 17 and 12 years of experience in tumour pathology, respectively, who were blinded to the results of MRE or other radiological assessments.

Statistical analysis

Continuous variables were analysed for normality using the Shapiro-Wilk test, and values (age, body mass index, and mass size) showing a normal distribution are expressed as means (±SD) and data showing non-normal distribution (stiffness measurements in different groups) are expressed as the median with 25th and 75th percentiles of the interquartile range

(IQR). Statistical comparisons were performed using student's *t*-test (age and BMI between control and patient groups) or Kruskal–Wallis H test with post-hoc Dunn's multiple comparisons test (mass stiffness, stiffness ratio and pancreatic parenchymal stiffness values among different groups), as appropriate. Categorical variables are expressed as counts and percentages. Chi-squared test (χ^2 test) was used to compare gender between control and patient groups. Intra- and inter-reader agreement were assessed using the intraclass correlation coefficients (ICC). Receiver operating characteristic (ROC) curve analyses were used to compare the diagnostic performance of mass stiffness, stiffness ratio and CA19-9 for differentiation between malignant (PDAC, metastatic tumour, and NEPT) and benign masses (MFP, lipoma, and SPN) and between PDAC and MFP. The area under the ROC curve (AUC), accuracy, sensitivity, specificity, negative predictive value (NPV), and positive predictive value (PPV) were then calculated. Comparisons of AUCs were done using the method proposed by DeLong et al [31]. Sensitivity, specificity, and accuracy were compared based on the McNemar test [32; 33]. Statistical analyses were performed with the commercially available SPSS Version 16.0J package (SPSS Inc, Chicago, IL). ROC curves and ROC curve comparisons were obtained with MedCalc software (MedCalc Software, Mariakerke, Belgium). $P<0.05$ indicated a significant difference.

RESULTS

Patients

The mean patient acceptance/comfort scores for MRE were 3.67±0.67 (patient group) and 4.05±0.60 (control group) (P=0.015). Except 4 patients who were excluded because of severe back pain, possibly secondary to neural invasion by tumour at the pancreatic body/tail, there were no complications of MRE reported during the study. There were no significant differences in age (student's t test, P=0.251), gender (Chi-squared test, P=0.299), or BMI (student's t test, P=0.365) between the patient and the control groups. Among the 85 patients, 53 underwent surgical resection of masses and were diagnosed by post-resection histological evaluation and 32 patients were diagnosed by EUS-FNA biopsy (details are presented in the Supplementary Appendix).

Stiffness of solid pancreatic masses and pancreatic parenchyma

The stiffness measurements for the masses showed excellent inter- and intra-reader agreement, with overall ICC values of 0.956 (95% confidence interval [CI]: 0.934–0.971) and 0.991 (95% CI: 0.987–0.994), respectively. Figure 2 and Figure 3 show representative MRE results for different solid pancreatic masses, and Figure 4 demonstrates 2 cases each of PDAC and MFP in which similar solid masses of the same subregions show widely divergent stiffness values.

Pancreatic stiffness in the control group was 1.21±0.12 kPa (range: 0.98 to 1.42 kPa). The stiffness of benign masses (median [IQR] = 1.96 [1.66–2.33] kPa) was significantly higher than that of healthy pancreas (Dunn's test, $P<0.001$) and lower than that of malignant masses (3.27 [2.43–4.38] kPa) (Dunn's test, $P<0.001$). The stiffness ratio of benign masses (median [IQR] = 1.14 [1.06–1.32]) was also significantly lower than that of malignant masses (2.38 [1.75–3.53], Mann-Whitney U test, $P<0.001$).

Mass stiffness, stiffness ratio and parenchymal stiffness values for different subtypes of masses are shown in Table 2 and Figure 5. When comparing the mass stiffness in PDAD/MFP/Metastasis/NEPT/SPN subtypes with normal pancreatic stiffness, the mass stiffness was significantly higher in each group except for SPN (Dunn's test, P<0.001, 0.003, 0.031, 0.001 and 0.41 respectively). The stiffness (median [IQR]= 3.30 [2.45–4.52] kPa) and stiffness ratio (2.45 [1.75–3.31]) in PDAC were similar to those of metastatic masses (Dunn's test, both P> 0.999) and were significantly higher than those of MFP (stiffness=2.00 [1.69–2.33] kPa, stiffness ratio=1.40 [1.06–1.22]; Dunn's test, both P<0.001). Both mass stiffness and stiffness ratio among cases of NEPT (range: 1.17–6.87 kPa and 1.19–7.01, respectively) and SPN (range: 1.05–4.87 kPa and 0.89–4.96, respectively) varied widely, showing no statistical difference to those of MFP (both P>0.999 for mass stiffness; P=0.249, P>0.999 for stiffness ratio, respectively).

The stiffness of the pancreatic parenchyma also showed significant variation among groups of different subtypes of masses (Kruskal-Wallis test, P<0.001; Table 2 and Figure 5C). Pancreatic parenchymal stiffness was greatest in MFP (1.72 [1.40, 2.02]kPa), followed by PDAC (1.45 [IQR:1.24,1.57] kPa; Dunn's test, P=0.479, without statistical significance) and then healthy pancreas (P<0.001 and P=0.002, respectively). Parenchymal stiffness in NEPT, metastatic tumour, and SPN was all similar to that of healthy pancreas (Dunn's test, all P>0.999).

Diagnostic performance

Table 3 summarises the performance of MRE vs CA19-9 for differentiation between benign and malignant tumours and between PDAC and MFP, with the AUC plots shown in Figure 6. Stiffness ratio showed better diagnostic performance for differentiation between benign and malignant masses than either mass stiffness or serum CA19-9 (AUC: 0.912 vs 0.845 vs 0.702; P=0.026 and P<0.001, respectively) and between PDAC and MFP (AUC: 0.955 vs 0.882 vs 0.745; P=0.026 and P=0.003, respectively). The stiffness ratio also showed better sensitivity (88.9% vs 68.5%, and 90.7% vs 72.1%; both P<0.001) than the mass stiffness in both tasks, while differences in specificity among the two measurements were not statistically significant (87.1% vs 93.5% and 95.8% vs 95.8%; both P>0.05).

The optimal cutoff value for the stiffness ratio, 1.38, provided a sensitive and specific indicator for differentiating malignancy from benign masses and PDAC from MFP. Among the 67 patients with confirmed PDAC or MFP, the stiffness ratio had an overall accuracy of 92.5% (62/67). Four of 43 cases of PDAC and 1 of 24 MFP cases were misclassified as the opposite category. Among all 85 of the pancreatic masses, 75 were correctly classified by the stiffness ratio for an overall accuracy rate of 88.2%. Four of 43 cases of PDAC, 1 of 24 cases of MFP, 2 of 7 cases of NEPT, and 3 of 6 cases of SPN were misclassified.

Discussion

Our preliminary results on a two-year prospective evaluation show that 3D SE-EPI MRE is well tolerated and feasible for assessing the mechanical properties for solid pancreatic masses. The diagnostic performance of the stiffness ratio was significantly better than either mass stiffness or serum CA19-9 level in differentiation of solid malignant tumours from

benign masses and, specifically, in differentiating PDAC from MFP. Sensitivity, specificity, and accuracy of the stiffness ratio for differentiation of PDAC from MFP were all >0.9.

Our finding that serum Ca19-9 had a high false-negative rate (sensitivity 46.5%) for predicting PDAC at an optimised cutoff value of 91 KU/L was in agreement with previous reports [13; 14]. The diagnostic performance of serum Ca19-9 was inferior to that of the MRE diagnostic indices in our evaluation, and our results showed that the MRE stiffness ratio (sensitivity 90.7%, specificity 95.8%) had comparable sensitivity but greater specificity than that reported for contrast-enhanced CT/MRI (sensitivity 82 to 94% and specificity 75 to 83%) [34; 35], and this result was comparable to the that of EUS elastography (sensitivity 100%, specificity 96.3%)[27; 36]. Microscopically, PDAC has obvious fibrous tissue infiltrating and enveloping the neoplasm [24], which could account for greater stiffness than both normal pancreas and MFP. MFP with various degrees of fibrosis was also shown to be stiffer than normal pancreas, and in some cases, overlapping the stiffness of PDAC, as shown both in our study and in previous EUS studies[37]. Since MFP always occurs in a background of chronic pancreatitis, which is expected to increase the referenced parenchymal stiffness, a change that would contribute to the lower stiffness ratio and tighter distribution of MFP and amplify its difference from PDAC. The parenchymal stiffness of PDAC is usually slightly higher than the normal pancreas, but not as high as MFP [38]. Thus, the diagnostic accuracy, sensitivity and NPV were all improved when adopting stiffness ratio.

EUS elastography has demonstrated as a promise technique for the differentiation between benign and malignant pancreatic masses, showing excellent sensitivity ranging from 95% to 100% and variable specificity ranging from 67% to 92.9% [27; 37]. We found that the MRE stiffness ratio achieved a reasonable sensitivity (88.9%) and specificity (87.1%) in differentiating benign and malignant pancreatic tumours. The slightly inferior performance of the MRE stiffness ratio when compared to EUS elastography, and in differentiating all tumours (malignancy from benignancy) vs PDAC from MFP can be explained by the wide range of stiffness values and the wide distribution of stiffness ratio in NEPT and SPN. Contrary to our results, NEPT and SPN showed a tight stiffness distribution at EUS elastography study [27], which may have contributed to better diagnostic performance in their study (sensitivity:100%, specificity:92.9%). This discrepancy will require additional evaluation in larger patient populations in each group, which would also improve the statistical power and clarify the true diagnostic potential of both stiffness and the stiffness ratio. In contrast to EUS elastography, MRE is noninvasive, and we did not encounter compression or motion artefacts from the vibration of the deep-seated pancreas. ROIs can be accurately drawn to exclude non-mass bearing tissues referencing magnitude images [29] and T2-weighted images, and MRE can be readily included in the standard pancreatic MRI protocol that is already in wide use in the management of patients with pancreatic disease. Hence, MRE can be recommended as a useful MR complementary sequence for differential diagnosis of solid pancreatic tumours.

This study has several limitations. Firstly, this is a single-centre study and the sample size is relatively small, particularly in terms of the number of patients with NEPT, SPN, and metastatic masses, and solid pancreatic tumours are not fully represented. Secondly, the

MRE technique has lower resolution than routine MRI. Although 3D SE-EPI MRE provides for clearer measurement of focal lesion stiffness and delineation of pancreatic and mass contour vs 2D gradient-recalled echo MRE, estimates based on lower frequencies may be biased in small masses because the special resolution is lower at 40 Hz than at 60 Hz. In the future, true 3D imaging may help improve the resolution and accuracy of MRE for focal lesions.

In conclusion, our preliminary results suggest that 3D SE-EPI MRE may have clinical applications for obtaining tissue stiffness measurements independent of morphological findings for characterisation and differentiation of solid pancreatic tumours. MRE is a relatively quick, effective, and promising method for non-invasive evaluation of solid pancreatic tumours, particularly in cases of PDAC vs MFP. We anticipate that our results will prompt further investigation in future studies.

Supplementary Material

Refer to Web version on PubMed Central for supplementary material.

Acknowledgments

Funding:

This study has received funding by the National Natural Science Foundation of China (No. 81401376, 81471718, 81271566), National Institutes of Health (grant EB001981), and Outstanding Youth Foundation of China Medical University (No. YQ20160005).

We thank Jun Chen, PHD, from the Department of Radiology, Mayo Clinic for his assistance with providing the tailored pancreatic MRE driver. We thank Bing Ma, from the Department of Clinical Epidemiology, Institute of Cardiovascular Diseases, and Center of Evidence Based Medicine, the First Affiliated Hospital of China Medical University, kindly provided statistical advice for this manuscript.

Abbreviations

MRE	MR elastography
CA19-9	carbohydrate antigen 19-9
PDAC	pancreatic ductal adenocarcinoma
MFP	mass-forming pancreatitis
ROC	receiver operating characteristic
AUC	area under the curve
SPN	solid pseudopapillary neoplasm
NEPT	neuroendocrine pancreatic tumour
CT	computed tomography
EUS	endoscopic ultrasound
EPI	echo planar imaging

FNA	fine-needle aspiration
3D	three dimensional
ROI	region of interest
SD	standard deviation
SE	spin echo
IQR	interquartile range
ANOVA	analysis of variance
ICC	intraclass correlation coefficient
NPV	negative predictive value
PPV	positive predictive value

References

1. Tokar JL, Walia R. Diagnostic evaluation of solid pancreatic masses. Curr Gastroenterol Rep. 2013; 15:347. [PubMed: 23996593]
2. Atwal T, Gleeson FC. Solid pancreatic masses: not always adenocarcinoma. Gastroenterol Hepatol (N Y). 2012; 8:853–854. [PubMed: 24693277]
3. Sunkara S, Williams TR, Myers DT, Kryvenko ON. Solid pseudopapillary tumours of the pancreas: spectrum of imaging findings with histopathological correlation. Br J Radiol. 2012; 85:e1140–1144. [PubMed: 22514105]
4. Kartalis N, Mucelli RM, Sundin A. Recent developments in imaging of pancreatic neuroendocrine tumors. Ann Gastroenterol. 2015; 28:193–202. [PubMed: 25830417]
5. Jemal A, Siegel R, Ward E, et al. Cancer statistics, 2008. CA Cancer J Clin. 2008; 58:71–96. [PubMed: 18287387]
6. Al-Hawary MM, Francis IR, Anderson MA. Pancreatic Solid and Cystic Neoplasms: Diagnostic Evaluation and Intervention. Radiol Clin North Am. 2015; 53:1037–1048. [PubMed: 26321452]
7. Braganza JM, Lee SH, McCloy RF, McMahon MJ. Chronic pancreatitis. Lancet. 2011; 377:1184–1197. [PubMed: 21397320]
8. de la Santa LG, Retortillo JA, Miguel AC, Klein LM. Radiology of pancreatic neoplasms: An update. World J Gastrointest Oncol. 2014; 6:330–343. [PubMed: 25232458]
9. Nichols MT, Russ PD, Chen YK. Pancreatic imaging: current and emerging technologies. Pancreas. 2006; 33:211–220. [PubMed: 17003640]
10. Frampas E, Morla O, Regenet N, Eugene T, Dupas B, Meurette G. A solid pancreatic mass: tumour or inflammation? Diagn Interv Imaging. 2013; 94:741–755. [PubMed: 23751230]
11. Baek JH, Lee JM, Kim SH, et al. Small (<or=3 cm) solid pseudopapillary tumors of the pancreas at multiphasic multidetector CT. Radiology. 2010; 257:97–106. [PubMed: 20663966]
12. Conwell DL, Lee LS, Yadav D, et al. American Pancreatic Association Practice Guidelines in Chronic Pancreatitis: evidence-based report on diagnostic guidelines. Pancreas. 2014; 43:1143–1162. [PubMed: 25333398]
13. Dranka-Bojarowska D, Lekstan A, Olakowski M, et al. The assessment of serum concentration of adiponectin, leptin and serum carbohydrate antigen-19.9 in patients with pancreatic cancer and chronic pancreatitis. J Physiol Pharmacol. 2015; 66:653–663. [PubMed: 26579571]
14. Ritchie SA, Chitou B, Zheng Q, et al. Pancreatic cancer serum biomarker PC-594: Diagnostic performance and comparison to CA19-9. World J Gastroenterol. 2015; 21:6604–6612. [PubMed: 26074698]

15. Merdrignac A, Sulpice L, Rayar M, et al. Pancreatic head cancer in patients with chronic pancreatitis. Hepatobiliary Pancreat Dis Int. 2014; 13:192–197. [PubMed: 24686547]
16. Glaser KJ, Manduca A, Ehman RL. Review of MR elastography applications and recent developments. J Magn Reson Imaging. 2012; 36:757–774. [PubMed: 22987755]
17. Shi Y, Guo Q, Xia F, et al. MR elastography for the assessment of hepatic fibrosis in patients with chronic hepatitis B infection: does histologic necroinflammation influence the measurement of hepatic stiffness? Radiology. 2014; 273:88–98. [PubMed: 24893048]
18. Cui J, Heba E, Hernandez C, et al. Magnetic resonance elastography is superior to acoustic radiation force impulse for the Diagnosis of fibrosis in patients with biopsy-proven nonalcoholic fatty liver disease: A prospective study. Hepatology. 2016; 63:453–461. [PubMed: 26560734]
19. Singh S, Venkatesh SK, Loomba R, et al. Magnetic resonance elastography for staging liver fibrosis in non-alcoholic fatty liver disease: a diagnostic accuracy systematic review and individual participant data pooled analysis. Eur Radiol. 2016; 26:1431–1440. [PubMed: 26314479]
20. Hennedige TP, Hallinan JT, Leung FP, et al. Comparison of magnetic resonance elastography and diffusion-weighted imaging for differentiating benign and malignant liver lesions. Eur Radiol. 2016; 26:398–406. [PubMed: 26032879]
21. Yoshimitsu K, Mitsufuji T, Shinagawa Y, et al. MR elastography of the liver at 3.0 T in diagnosing liver fibrosis grades; preliminary clinical experience. Eur Radiol. 2016; 26:656–663. [PubMed: 26060066]
22. Schober M, Jesenofsky R, Faissner R, et al. Desmoplasia and chemoresistance in pancreatic cancer. Cancers (Basel). 2014; 6:2137–2154. [PubMed: 25337831]
23. Imamura T, Iguchi H, Manabe T, et al. Quantitative analysis of collagen and collagen subtypes I, III, and V in human pancreatic cancer, tumor-associated chronic pancreatitis, and alcoholic chronic pancreatitis. Pancreas. 1995; 11:357–364. [PubMed: 8532652]
24. Armstrong T, Packham G, Murphy LB, et al. Type I collagen promotes the malignant phenotype of pancreatic ductal adenocarcinoma. Clin Cancer Res. 2004; 10:7427–7437. [PubMed: 15534120]
25. Witt H, Apte MV, Keim V, Wilson JS. Chronic pancreatitis: challenges and advances in pathogenesis, genetics, diagnosis, and therapy. Gastroenterology. 2007; 132:1557–1573. [PubMed: 17466744]
26. Kelly KA, Hollingsworth MA, Brand RE, et al. Advances in Biomedical Imaging, Bioengineering, and Related Technologies for the Development of Biomarkers of Pancreatic Disease: Summary of a National Institute of Diabetes and Digestive and Kidney Diseases and National Institute of Biomedical Imaging and Bioengineering Workshop. Pancreas. 2015; 44:1185–1194. [PubMed: 26465948]
27. Iglesias-Garcia J, Larino-Noia J, Abdulkader I, Forteza J, Dominguez-Munoz JE. Quantitative endoscopic ultrasound elastography: an accurate method for the differentiation of solid pancreatic masses. Gastroenterology. 2010; 139:1172–1180. [PubMed: 20600020]
28. Kim SY, Cho JH, Kim YJ, et al. Diagnostic efficacy of quantitative endoscopic ultrasound elastography for differentiating pancreatic disease. J Gastroenterol Hepatol. 2016; doi: 10.1111/jgh.13649
29. Shi Y, Glaser KJ, Venkatesh SK, Ben-Abraham EI, Ehman RL. Feasibility of using 3D MR elastography to determine pancreatic stiffness in healthy volunteers. J Magn Reson Imaging. 2015; 41:369–375. [PubMed: 24497052]
30. Chari ST. Chronic pancreatitis: classification, relationship to acute pancreatitis, and early diagnosis. J Gastroenterol. 2007; 42(Suppl 17):58–59. [PubMed: 17238029]
31. DeLong ER, DeLong DM, Clarke-Pearson DL. Comparing the areas under two or more correlated receiver operating characteristic curves: a nonparametric approach. Biometrics. 1988; 44:837–845. [PubMed: 3203132]
32. Hanley JA, McNeil BJ. A method of comparing the areas under receiver operating characteristic curves derived from the same cases. Radiology. 1983; 148:839–843. [PubMed: 6878708]
33. Obuchowski NA, McClish DK. Sample size determination for diagnostic accuracy studies involving binormal ROC curve indices. Stat Med. 1997; 16:1529–1542. [PubMed: 9249923]

34. Yamada Y, Mori H, Matsumoto S, Kiyosue H, Hori Y, Hongo N. Pancreatic adenocarcinoma versus chronic pancreatitis: differentiation with triple-phase helical CT. Abdom Imaging. 2010; 35:163–171. [PubMed: 19771464]

35. Adamek HE, Albert J, Breer H, Weitz M, Schilling D, Riemann JF. Pancreatic cancer detection with magnetic resonance cholangiopancreatography and endoscopic retrograde cholangiopancreatography: a prospective controlled study. Lancet. 2000; 356:190–193. [PubMed: 10963196]

36. Iglesias Garcia JJ, Larino Noia J, Alvarez Castro A, Cigarran B, Dominguez Munoz JE. Second-generation endoscopic ultrasound elastography in the differential diagnosis of solid pancreatic masses. Pancreatic cancer vs. inflammatory mass in chronic pancreatitis. Rev Esp Enferm Dig. 2009; 101:723–730. [PubMed: 19899942]

37. Kawada N, Tanaka S. Elastography for the pancreas: Current status and future perspective. World J Gastroenterol. 2016; 22:3712–3724. [PubMed: 27076756]

38. Park MK, Jo J, Kwon H, et al. Usefulness of acoustic radiation force impulse elastography in the differential diagnosis of benign and malignant solid pancreatic lesions. Ultrasonography. 2014; 33:26–33. [PubMed: 24936492]

Key points

1. 3D SE-EPI MRE is useful for calculating stiffness of solid pancreatic tumours.
2. Stiffness ratio outperformed mass stiffness and CA19-9 for differentiating PDAC and MFP.
3. Incorporation of 3D SE-EPI MRE into a standard MRI protocol is recommended.

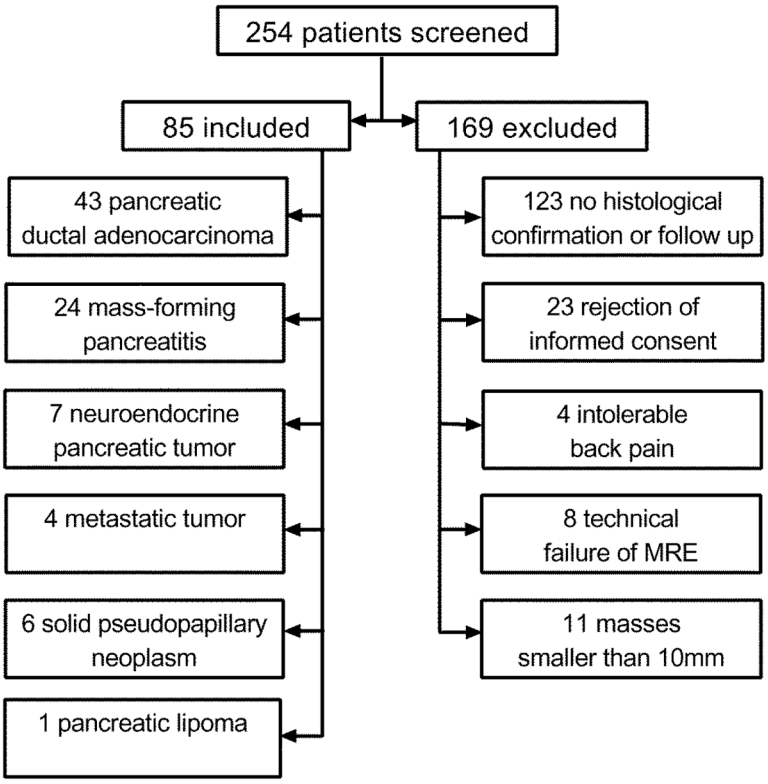

Figure 1.
Flowchart shows the study enrolment process during the 24-month study period

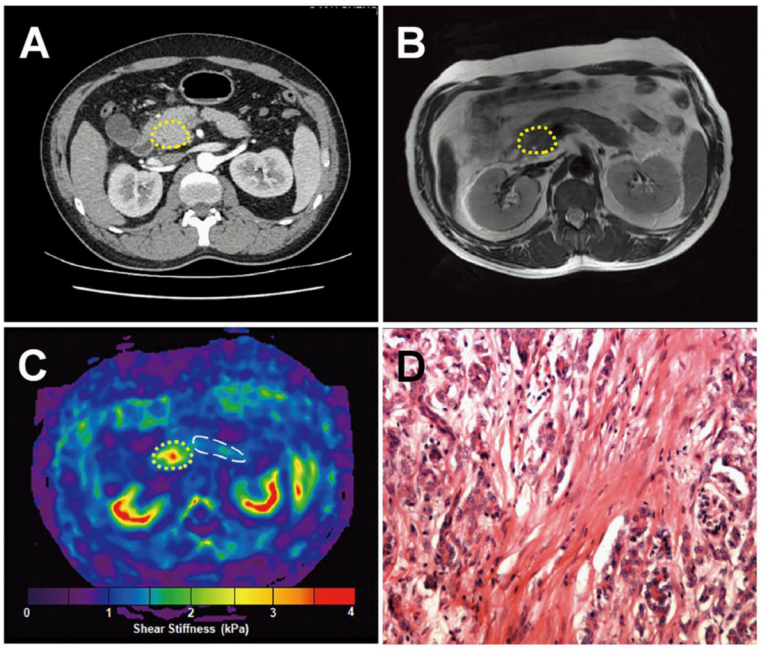

Figure 2.

A 62-year-old man with mass-forming pancreatitis. **a**. Axial contrast-enhanced CT image shows an ill-defined isodense mass at the head of the pancreas. **b**. The mass appears almost isointense in axial T2-weighted MR images. **c**. In the elastogram, the lesion appears to be stiffer than the surrounding pancreatic parenchyma (2.43±0.48 kPa vs 1.27±0.42 kPa). The placement of regions of interest (ROI) is shown in both the tumour and pancreatic parenchyma, encompassing the mass and the parenchyma, excluding boundaries, large vessels, and surrounding tissues. **d**. Histological sections (haematoxylin-eosin stain, ×10) confirmed benign mass-forming pancreatitis.

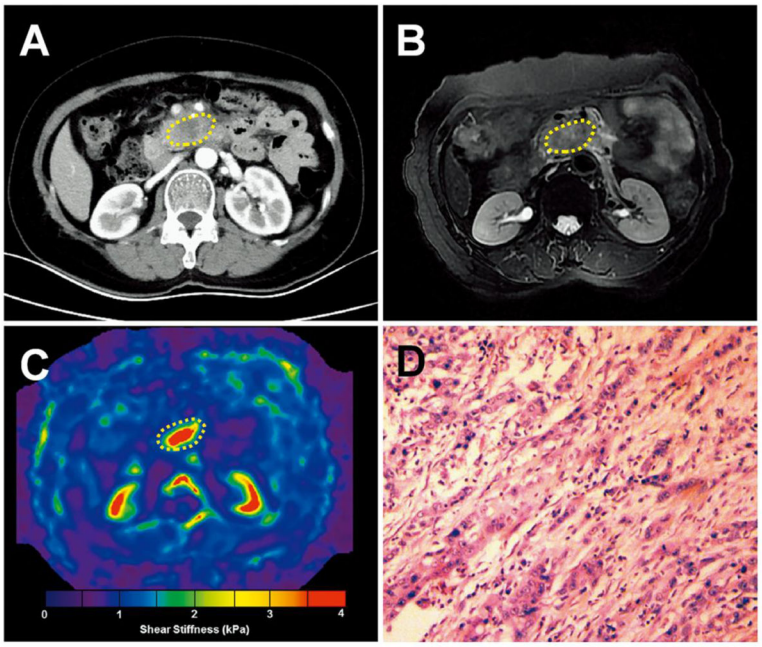

Figure 3.

A 56-year-old woman with pancreatic adenocarcinoma. **a**. Axial contrast-enhanced CT image shows an ill-defined hypodense mass in the uncinate process. **b**. The mass is slightly hyperintense or isointense in axial fat-saturated T2-weighted MR images. **c**. In the MRE elastogram, the lesion is much stiffer than the surrounding tissue (3.30 ± 0.98 kPa vs 1.37± 0.33 kPa). **d**. Histological sections (haematoxylin-eosin stain, ×10) confirmed a moderately differentiated pancreatic adenocarcinoma.

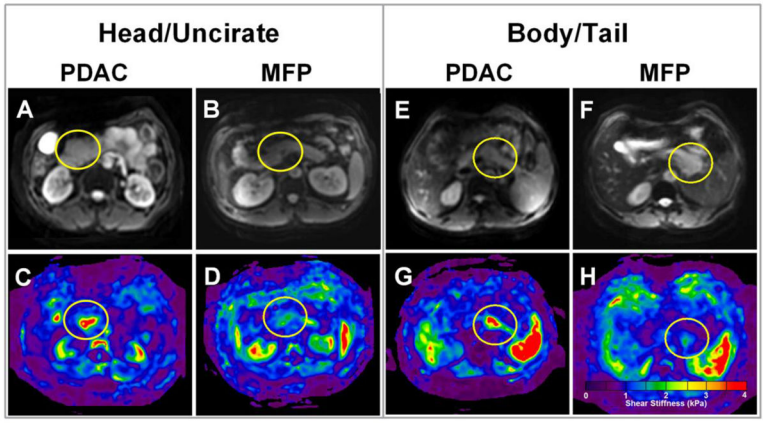

Figure 4.

Pancreatic ductal adenocarcinoma (PDAC) and mass-forming pancreatitis (MFP) with similar imaging features but very different stiffness values at MR elastography. **a–d.** The magnitude images (a, b) show (a) PDAC and (b) MFP presenting as similar solid masses at the pancreatic head/uncinate process. The elastograms (c, d) show that the PDAC had a much greater stiffness than the MFP (mean stiffness: 2.95± 0.81 kPa vs 1.65±0.57 kPa). **e–h.** Magnitude images of cases of (e) PDAC and (f) MFP at the body/tail also show similar solid masses, and, likewise, the elastograms (g, h) showed that the PDAC had much higher stiffness than the MFP (mean stiffness: 2.84±1.23 kPa vs 1.35± 0.47 kPa).

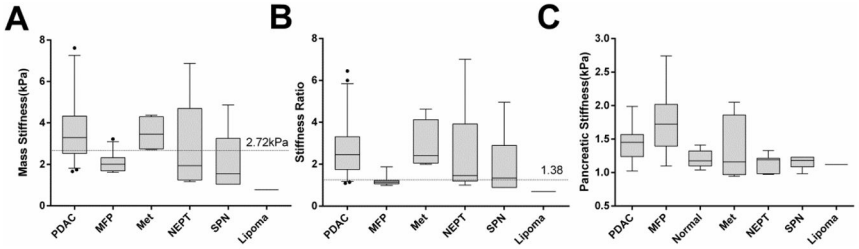

Figure 5.

The distributions of pancreatic mass stiffness (a), stiffness ratio (b) and the parenchymal stiffness (c) for various of solid pancreatic masses including benign mass-forming pancreatitis (MFP), pancreatic adenocarcinoma (PDAC), neuroendocrine pancreatic tumour (NEPT), metastatic tumour (Met), solid pseudopapillary neoplasm (SPN), lipoma, and normal pancreas. The stiffness ratio (b) was calculated as the ratio of the stiffness of the mass (a) to the stiffness of the non-mass-bearing pancreatic parenchyma (c). The median, quartiles, and 95% confidence intervals (CI) of different groups are also shown. An outlier in the PDAC group with the highest stiffness (10.64 kPa) is not shown (a). The two horizontal lines in (a) and (b) correspond to the cutoffs obtained from area under the receiver operator characteristic curve analysis.

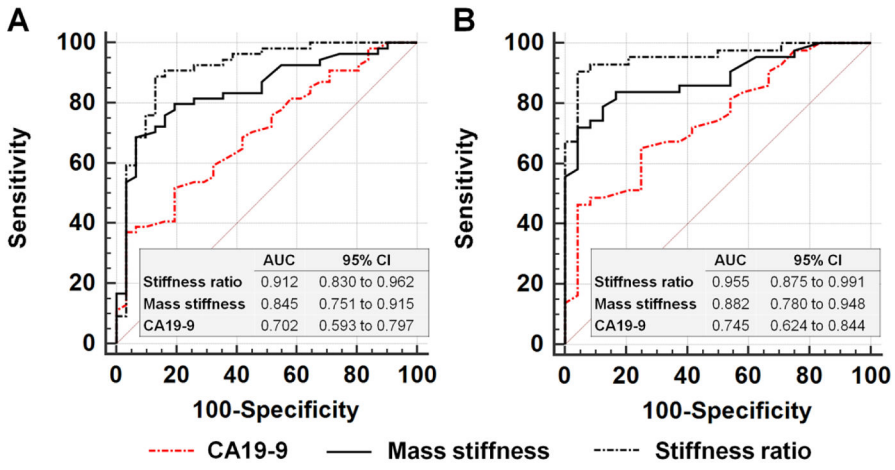

Figure 6.

Composite graph comparing the receiver operating characteristic (ROC) curves for serum CA19-9 levels, mass stiffness, and stiffness ratio (mass stiffness/parenchymal stiffness). **a**. Differentiation of malignant from benign pancreatic masses and **b**. differentiation of pancreatic adenocarcinoma from mass-forming pancreatitis. The numbers in the tables indicate area under the ROC curve (AUC) values and 95% CIs. All of the pairwise comparisons of the AUCs in a and b were significant, as follows. a: CA19-9 vs mass stiffness, P=0.048; CA19-9 vs stiffness ratio, P<0.001; stiffness ratio vs mass stiffness, P=0.026. b: CA19-9 vs mass stiffness, P=0.038; CA19-9 vs stiffness ratio, P=0.003; stiffness ratio vs mass stiffness, P=0.026.

Table 1

Baseline Characteristics and MRE Stiffness Measurements of 85 Patients with Solid Pancreatic Masses

Characteristics	All Patients	Benign (n=31)	Malignant (n=54)
Sex (M/F)	58/27	20/11	38/16
Age (years)	54.0±12.1	47.6±13.6	57.7±9.5
BMI (kg/m^2)	21.1±2.7	22.4±2.5	20.4±2.6
Head/body/tail	50/21/14	19/8/4	31/13/10
Size (mm)	37.2±17.9	35.4±21.2	38.3±15.9
Serum CA19-9 (KU/L)	64 (39–98)	52 (24–73)	75(48–121)
Serum amylase (U/L)	72 (41–125)	39 (22–54)	98 (60–136)
Serum lipase (U/L)	11.2 (3.5–22)	4.0 (2.9–11.1)	13.9 (5.9–22.4)
TBIL (μmol/L)	12.2 (4.2–64.3)	11.2 (2.5–23.1)	17.9 (5.1–65.5)
DBIL (μmol/L)	5.5 (3.2–27.5)	4.5 (2.4– 5.8)	11.3 (4.3–29.9)
FBG (mmol/L)	5.2 (4.1–7.1)	5.1 (4.7–6.9)	5.4 (3.9–7.1)

Continuous data are presented as median (25th–75th percentiles) or mean ± standard deviation. *TBIL* total bilirubin; *DBIL* direct bilirubin; *FBG* fasting blood glucose.

Table 2

MRE Stiffness Measurements of Patients with Different Types of Solid Pancreatic Masses

Mass	Mass stiffness (kPa)	Stiffness ratio	Parenchymal stiffness (kPa)
PDAC (n=43)	3.30 (2.45–4.52)	2.45 (1.75–3.31)	1.45 (1.24,1.57)
MFP (n=24)	2.00 (1.69–2.33)	1.40 (1.06–1.22)	1.72 (1.40,2.02)
NEPT (n=7)	2.32 (1.42–5.69)	2.09 (1.21–4.70)	1.19 (0.98,1.21)
Met (n=4)	3.46 (2.75–4.30)	2.42 (2.05–4.13)	1.18 (1.09,1.23)
SPN (n=6)	1.55 (1.05–3.26)	1.33 (0.89–2.90)	1.16 (0.97,1.57)
Lipoma (n=1)	0.78	0.7	1.121
P value	<0.001	<0.001	<0.001

Continuous data are presented as medians (25th to 75th percentiles). *PDAC* pancreatic adenocarcinoma; *MFP* mass-forming pancreatitis; *NEPT* neuroendocrine pancreatic tumour; *Met* metastasis; *SPN* solid pseudopapillary neoplasm. The P-values were calculated by Kruskal-Wallis H test (excluding the lipoma). By using post-hoc Dunn's multiple comparisons test, the following pairwise comparisons showed statistical difference: PDAC vs MFP (P<0.001) and PDAC vs SPN (P=0.039) for mass stiffness; PDAC vs MFP (P<0.001) and MFP vs Met (P=0.018) for stiffness ratio.

Table 3

Performance of MRE for diagnosing Malignant from Benign Masses in 85 patients, and diagnosing Pancreatic Ductal Adenocarcinoma (PDAC) from Mass-Forming Pancreatitis (MFP) in 67 patients

Prediction	**Malignant vs benign masses**			**PDAC vs MFP**		
Parameters	**Mass stiffness**	**Stiffness ratio**	**CA19-9**	**Mass stiffness**	**Stiffness ratio**	**CA19-9**
Cutoff	2.72kPa	1.38	91 KU/L	2.72kPa	1.38	91 KU/L
AUC	0.845 (0.751–0.915)	0.912 (0.830–0.962)	0.702 (0.593–0.797)	0.882 (0.780–0.948)	0.955 (0.875–0.991)	0.745 (0.624–0.844)
Sensitivity (%)	68.5 (54.4–80.5)	88.9 (77.4–95.8)	37.0 (24.3–51.3)	72.1 (56.3–84.7)	90.7 (77.9–97.4)	46.5 (31.2–62.3)
Specificity (%)	93.5 (78.6–99.2)	87.1 (70.2–96.4)	96.8 (83.3–99.9)	95.8 (78.9–99.9)	95.8 (78.9–99.9)	95.8 (78.9–99.9)
PPV (%)	94.9 (82.7–99.4)	92.3 (81.5–97.9)	95.2 (76.2–99.9)	96.9 (83.8–99.9)	97.5 (86.8–99.9)	95.2 (76.2–99.9)
NPV (%)	63.0 (47.5–76.8)	81.8 (64.5–93.0)	46.9 (34.3–59.8)	65.7 (47.8–80.9)	85.2 (66.3–95.8)	50.0 (34.9–65.1)
Accuracy (%)	77.6	88.2	58.8	80.5	92.5	64.2

Cut-off values were selected based on receiver operating characteristic (ROC) analysis with greater stiffness/stiffness ratio in PDAC/malignancy. Numbers in parentheses are the 95% confidence interval. *AUC* area under the ROC curve; *NPV* negative predictive value; *PPV* positive predictive value.